

NASA Technical Memorandum 81360

Comparison of Three Thrust Calculation Methods Using In-Flight Thrust Data

Donald L. Hughes
Dryden Flight Research Center
Edwards, California



**Scientific and Technical
Information Branch**

1981

COMPARISON OF THREE THRUST CALCULATION METHODS USING IN-FLIGHT THRUST DATA

Donald L. Hughes
Dryden Flight Research Center

INTRODUCTION

Various methods have been devised to calculate jet engine gross thrust. If an absolute value of engine gross thrust is required with a relatively high degree of accuracy, the engine must be heavily instrumented and calibrated in an altitude facility. If an absolute value of engine gross thrust is not required, calculation methods can be employed that use less engine instrumentation and do not require altitude-facility testing.

The KC-135A winglets flight program conducted at the NASA Dryden Flight Research Center required the determination of the difference in total aircraft drag with and without the winglets installed. To determine this difference in total aircraft drag, repeatable values of calculated jet engine gross thrust were required. Absolute values of gross thrust were not required for this flight program. However, since the engines were to be instrumented to obtain thrust, and a series of thrust stand calibrations were to be performed for the winglet program, an opportunity existed to compare the characteristics of three methods for calculating engine gross thrust. The three methods were: (1) the gas generator method (GGM, ref. 1), (2) the mass momentum method (MMM, ref. 2), and (3) the simplified gross thrust method (SGTM, refs. 3 and 4).

The GGM was used as a baseline for the comparisons in this report, since it was the technique used by the engine manufacturer. It should be noted that because of the simplicity of the nonafterburning engine used in this investigation, the three methods, which are different in concept, were not totally independent.

The approach taken in this investigation was to use the thrust stand data to adjust the three methods through coefficients to the thrust-stand-measured values and then to extrapolate the coefficients to cruise flight conditions. The adjustment procedures are described in appendix A. A comparison could then be made of cruise flight thrust as determined from the three methods.

This report documents the three thrust calculation methods and summarizes the results obtained when data from an aircraft with simple nonafterburning turbojet engines are processed through these calculation methods. A comparison is made of the characteristics of the three techniques at several stabilized airspeeds at high altitudes ranging from 10,342 meters (33,930 feet) to 11,814 meters (38,670 feet) over a range of Mach numbers from 0.62 to 0.82.

SYMBOLS AND ABBREVIATIONS

Physical quantities in this report are given in the International System of Units (SI) and parenthetically in U.S. Customary Units. The measurements were taken in U.S. Customary Units.

A	area, m^2 (ft^2)
$\frac{dA}{A}$	cross-sectional area change term
C_f	nozzle flow coefficient
C_{fg}	conventional gross thrust coefficient
C_{gp}	gross thrust coefficient
C_{gp}'	gross thrust coefficient, adjusted
F_g	gross thrust, N (lb)
GGM	gas generator method
g_0	gravitational constant, $6.6732 \times 10^{-11} \text{ N m}^2 \text{ kg}^{-2}$ ($32.17 \text{ ft-lb/lb-sec}^2$)
h	altitude, m (ft)
K_2	adjustment factor, SGTM
M	Mach number
MMM	mass momentum method

$\frac{dM}{M}$	momentum change term of frictional effects
\dot{m}	mass flow, kg/sec (lbm/sec)
$N_1/\sqrt{\theta_{t_2}}$	corrected low compressor rotor speed, rpm
p	pressure, kN/m ² (psi)
$\frac{dp_t}{p_t}$	total pressure change term
R_g	gas constant, $8.314 \times 10^3 \text{ J kmol}^{-1} \text{ K}^{-1}$ (53.35 ft-lbf/lbm-°R)
SGTM	simplified gross thrust method
T	temperature, K (°R)
$\frac{dT_t}{T_t}$	total temperature change term
V	velocity, m/sec (ft/sec)
W/δ	weight-pressure parameter, kg (lb)
γ	ratio of specific heats
ρ	density, kg/m ³ (lbm/ft ³)
ψ	gross thrust parameter
$\frac{d\omega}{\omega}$	mass flow change term

Subscripts:

amb	ambient conditions
c	calculated
F	engine station inside nozzle exit
m	measured
ref	reference conditions
s	static

t	total
2	compressor face engine station
7	turbine discharge engine station
8	nozzle discharge engine station
∞	free stream

DESCRIPTION OF APPARATUS

Airplane

The KC-135A aircraft is used primarily as a high altitude refueling tanker. The aircraft was modified for the winglet research program by the installation of aerodynamically shaped winglets mounted on the wingtips (fig. 1). These winglets were adjustable in both incidence angle and cant angle (the angles around the vertical axis and from the vertical plane, respectively). The KC-135A aircraft was flown without the winglets installed to establish a baseline drag level. The aircraft was then flown again over the same flight conditions with the winglets installed to obtain the change in drag.

Propulsion System

The KC-135A aircraft was powered by four Pratt & Whitney J57-P-43W engines. This engine was a continuous flow turbojet engine with a 16-stage low and high pressure axial flow compressor driven by a 3-stage low and high pressure reaction turbine (fig. 2). The engine had a fixed area primary exhaust nozzle and no afterburner. The engines were rated (uninstalled) at 49,820 newtons (11,200 pounds) of thrust for military power operation at standard sea level static conditions. Water injection was available for takeoff, but was never used during tests at altitude.

TEST PROCEDURE

Thrust Stand Calibration

Thrust measurements were made during ground tests with the airplane installed in the Edwards Air Force Base static thrust calibration facility. This facility consists of four platforms, each of which measures applied force. For these tests, the airplane was positioned with both main landing gear wheels on the center platform and the nose gear wheels on the forward platform. The tests consisted of stabilized runs at various power settings on pairs of engines (both inboard or both outboard) and with all engines operating. The same thrust values measured during this ground calibration were used to adjust all three gross thrust calculation procedures so that

calculated gross thrust would be equal to measured gross thrust over the range of thrust available on the ground. A description of the adjustment procedure is given in appendix A.

Flight Test Procedure

Flight data were obtained at several stabilized airspeeds at altitudes ranging from 10,342 meters (33,930 feet) to 11,814 meters (38,670 feet) (table 1). Mach number varied from 0.62 to 0.82.

INSTRUMENTATION

Figure 2 shows the location of the instrumentation and station designations for the J57-P-43W turbofan engine. Conventional probes connected by tubes to remotely located transducers were installed in rakes at the compressor face of engines 1 and 2 (left side). Differential pressure transducers were used to measure all engine and compressor face (p_{t_2}) total pressures. Reference pressure was obtained from a

probe located at the compressor face of engine number 2. This probe pressurized a tank that was monitored by a highly accurate absolute pressure transducer. The engine pressures measured consisted of turbine discharge total pressure (p_{t_7}); nozzle discharge static pressure (p_{s_F}); nozzle discharge total pressure (p_{t_F}) (engine number 2 only); and compressor face static pressure (p_{s_2}). Engine rotor speeds, throttle compressor bleed positions, fuel flow rates, and fuel temperature were also measured. Other parameters obtained were Mach number, altitude, angle of attack, angle of sideslip, ambient air temperature, aircraft accelerations, control surface positions, and fuel used. The precision of the important measured and derived quantities is given in table 2. Zero and power supply voltage corrections and calibrations were applied to all parameters when converting the digital pulse code modulation (PCM) data into engineering units.

THRUST CALCULATIONS

Gas Generator Method

The GGM, which is known as a pressure-area method for the calculation of engine thrust, was used as the baseline for this report. The method was developed by the engine manufacturer and is explained in reference 1. The basic equation for the method is

$$F_g = \psi p_{amb} C_{gp} A_8$$

where:

ψ function of p_{t_7}/p_{amb} and γ

C_{gp} function of p_{t_7}/p_{amb} (manufacturer's curve adjusted by static thrust calibration)

A_8 nozzle area

γ ratio of specific heat of gas function of T_{t_7}

The thrust stand data were used to make calculated gross thrust equal to measured gross thrust by adjusting the C_{gp} curve for an average uninstalled J57-P-43W engine (fig. 3 and app. A).

Mass Momentum Method

Another method available for the calculation of gross thrust is referred to here as the MMM (ref. 2). This calculation procedure determines the force caused by the change in momentum of the fluids passing through the engine and is essentially another pressure-area method. The basic equation for the method is

$$F_g = C_f A_8 \left[\left(\frac{2}{\gamma + 1} \right)^{\frac{\gamma}{\gamma - 1}} (\gamma + 1) p_{t_7} - p_{amb} \right]$$

where:

C_f nozzle coefficient

A_8 nozzle area

p_{t_7} total pressure at turbine exit

γ ratio of specific heat of gas

If the ratio of specific heat of gas is assumed to be 1.33,

$$F_g = C_f A_8 (1.259 p_{t_7} - p_{amb})$$

The values of gross thrust as calculated by the MMM are for a theoretical engine obeying the perfect gas laws on the assumption that the ratio of specific heats (γ) is constant for a nonafterburning engine. Because the jet exhaust nozzle is not perfect, and because it is necessary to compensate for instrumentation and installation effects, the calculated gross thrust was adjusted by a nozzle coefficient C_f . This coefficient was determined during the static ground thrust calibration run as a function of p_{t_7}/p_{amb} over the range of p_{t_7}/p_{amb} available on the ground (fig. 4). See appendix A for the development of C_f .

Simplified Gross Thrust Method

The third procedure for calculating engine gross thrust, which is in effect a third pressure-area method, was originally developed as a means of calculating a value of thrust given only measured engine parameters at the engine exit. The analytical procedure was originally used to calculate the thrust of a more complicated jet engine that incorporated afterburners, ducted fans, and so forth. The original equation is described in references 3 and 4. The modified equations used for this study are shown below; their derivation is given in appendix B.

$$F_g = \left(\frac{2\gamma_F}{\gamma_F - 1} \right) A_F p_s F \left(\frac{p_{t_F}}{p_{s_F}} \right)^{\frac{\gamma_F - 1}{2\gamma_F}} \sqrt{\left(\frac{p_{t_F}}{p_{s_F}} \right)^{\frac{\gamma_F - 1}{\gamma_F}} - 1} \sqrt{1 - \left(\frac{p_{s_{amb}}}{p_{t_F}} \right)^{\frac{\gamma_F - 1}{\gamma_F}}}$$

For the unchoked nozzle, this equation is valid whenever

$$\frac{p_{t_F}}{p_{s_{amb}}} < \left(\frac{\gamma_F - 1}{2} \right)^{\frac{\gamma_F}{\gamma_F - 1}}$$

and

$$T_{t_7} \leq 700^\circ R, \gamma_F = 1.4$$

or

$$T_{t_7} > 700^\circ R, \gamma_F = 2.246409 \left(T_{t_7} \right)^{-0.070767}$$

The value of p_{t_F} is calculated as follows:

$$p_{t_F} = p_{t_7} \left\{ 1 - \left(\frac{\gamma_F}{\gamma_F - 1} \right) K_2 \left[\left(\frac{p_{t_7}}{p_{s_F}} \right)^{\frac{\gamma_F - 1}{\gamma_F}} - 1 \right] \right\}$$

The K_2 adjustment factor used in the last equation is discussed in appendix B.

The nozzle is considered choked whenever

$$\frac{p_{t_F}}{p_{s_F}} \geq \left(\frac{\gamma_F - 1}{2} \right)^{\frac{\gamma_F}{\gamma_F - 1}}$$

The equation then becomes

$$F_g = \left(\frac{2\gamma_F}{\gamma_F - 1} \right) A_F p_{s_F} \sqrt{\left[\left(\frac{p_{t_F}}{p_{s_F}} \right)^{\frac{\gamma_F - 1}{\gamma_F}} - 1 \right]} \left(\frac{p_{t_F}}{p_{s_F}} \right)^{\frac{\gamma_F - 1}{2\gamma_F}} \left\{ \sqrt{\frac{\gamma_F - 1}{\gamma_F + 1}} \right. \\ \left. + \frac{\sqrt{\frac{\gamma_F - 1}{2}}}{\gamma_F} \left[\left(\frac{2}{\gamma_F + 1} \right)^{\frac{\gamma_F}{\gamma_F - 1}} - \frac{p_{s_{amb}}}{p_{t_F}} \right] \left(\frac{\gamma_F + 1}{2} \right)^{\frac{\gamma_F + 1}{2(\gamma_F - 1)}} \right\}$$

The adjustment of calculated gross thrust to equal measured gross thrust occurs in the determination of p_{t_F} , which is not a measured parameter. The empirical equation which determines p_{t_F} has an adjustment factor K_2 which is iterated until a match is obtained between calculated and measured gross thrust from the ground thrust calibration data (app. B).

Comparison of the Three Methods

Table 3 compares the parameters required in the final expression for the application of the three methods to the J57 engine and identifies the constants, variables, and coefficients used. As the table shows, all three methods use an adjusting coefficient, but the MMM is unique in that it has no variables. The MMM

also uses a constant value of γ , whereas the other methods incorporate γ as a function of T_{t_7} . The GGM requires the use of an engine manufacturer's curve that

was empirically developed and flight test verified for a standard engine in the determination of C_{gp} , and it is dependent upon this curve plus a calibration adjustment to calculate engine gross thrust. The SGTM relies upon a static measurement near the nozzle discharge exit, p_{s_F} , and all of the empirical calculations are adjusted to

this measurement location. Since all three calculation methods used essentially the same parameters, the same data, and are essentially pressure-area methods, the calculated thrust values obtained from each of the three methods should be comparable and the same relationships should be maintained over the range of thrust evaluated.

RESULTS AND DISCUSSION

Because the flight data used in the calculation of gross thrust for each of the three calculation procedures came from the same instrumentation and the same flight maneuvers, the calculated gross thrust from each of the stabilized flight data points is directly comparable. For the data from flights separated by varying time intervals to be comparable, it is necessary for the engines to have remained in comparable condition, because engine deterioration causes changes in basic engine relationships. The condition of an engine can be monitored by the continual evaluation of certain engine parameters, such as corrected rpm versus engine pressure ratio, p_{t_7}/p_{t_2}

(fig. 5). The data shown in figure 5 were obtained during five flights, including the first and last flights for which thrust data were acquired. The engines and instrumentation used to obtain the data appear to have remained in good condition, with no adverse trends apparent in any of the four engines for any of the flights.

The values of gross thrust calculated with all three methods are compared in figure 6 for each of the four engines for all of the performance flights. The circle symbols show the percentage of difference between the thrust values calculated by the MMM and those calculated by the GGM. If the two methods had calculated the same value of gross thrust, the data would have fallen on the lines of 0 percent difference. Actually the MMM calculated a larger gross thrust value than the GGM by 1.5 to 2.5 percent over the range of thrust evaluated for engines 1, 3, and 4. Engine 2 differed by 2.75 to 3.75 percent. The square symbols denote a comparison of the thrust values calculated by the SGTM with the values calculated by the GGM. The SGTM calculated a gross thrust value that was less than the value calculated by the GGM by 1 to 2.75 percent over the range of thrust evaluated for engine numbers 1, 2, and 3. Engine 4 differed by 2.25 to 3.75 percent over the range of thrust evaluated. This was the first time the SGTM had ever been used to calculate thrust for a nonafterburning engine with a short tailpipe, and this method showed the same consistency in results as the other two methods.

In calculating the total gross thrust for the airplane, the thrust values from all four engines are combined, and this tends to remove the differences between the individual engines. The calculated gross thrust value of all four engines combined is compared for the three calculation methods in figure 7. The values of total gross

thrust as calculated by the MMM are between 1.75 and 2.75 percent higher than those values calculated by the GGM over the tested range of thrust. The values of total gross thrust as calculated by the SGTM are 1.50 to 2.50 percent lower than the values calculated by the GGM. The difference between the calculated values of gross thrust for the three methods remained nearly constant, or biased; that is, they maintained the same relationship within ± 0.5 percent (the change in bias appears ordered) over the range of thrust. In other words, if the nearly constant bias could be removed somehow, the values of thrust calculated by the three methods would overlie each other within ± 0.5 percent. In the case of the MMM, the extrapolation of the nozzle coefficient, C_f , was suspected of being the cause of the bias; consequently, the nozzle coefficient was re-extrapolated in such a way that the curve reached a maximum value of 0.915 (fig. 8) instead of 0.930 (fig. 4). When thrust values were calculated with the MMM and the revised curve and then compared with the values calculated with the GGM, the results shown in figure 9 were produced. At the highest levels of gross thrust, the values of thrust calculated by the two methods for three of the engines converged, and at the lower levels of gross thrust the differences between the values were still approximately 1 percent. Thus, by simply re-extrapolating the C_f curve, the values of gross thrust as calculated by the two methods were made to agree more closely; the change in bias over the range of thrust increased but was still ordered.

An attempt was made to adjust the K_2 factor for the SGTM and to reduce the difference between the values of gross thrust calculated by the GGM and the SGTM. However, it was impossible to come up with an adjustment that was logical and worked with both the ground thrust data and the flight-derived data.

The coefficients from each of the calculation methods were adjusted to make the calculated data agree with the measured data during the thrust stand calibration and then were extrapolated to cruise flight conditions. Agreement between values of in-flight thrust data as calculated by the three methods was found to be within ± 3 percent in total aircraft gross thrust.

CONCLUSIONS

The gross thrust of an experimental airplane was calculated by three different, but not totally independent, methods. A comparison of the values of gross thrust computed by the three calculation methods led to the following conclusions:

1. With the coefficients for the aircraft determined from thrust stand calibrations and extrapolated to cruise flight conditions, agreement between methods was found to be within ± 3 percent in total aircraft gross thrust.
2. The disagreement in the calculated thrust values produced by the different calculation techniques manifested itself as a bias in the data. The scatter in the calculated data for the thrust levels examined in flight was small (± 0.5 percent).

*Dryden Flight Research Center
National Aeronautics and Space Administration
Edwards, Calif., April 29, 1981*

APPENDIX A.—CALCULATION ADJUSTMENT PROCEDURES
USING GROUND THRUST CALIBRATIONS

Each of the thrust calculation methods required an adjustment to make calculated gross thrust equal to measured gross thrust. The adjustment procedures are given below.

Gas Generator Method

The gross thrust coefficient (C_{gp}) curve for an average uninstalled J57-P-43W engine is furnished by the engine manufacturer. This C_{gp} curve is a function of p_{t_7}/p_{amb} and is adjusted after making a ground static thrust run while measuring gross thrust, p_{amb} , and all of the required engine parameters. The corrected C_{gp} , or C_{gp}' , is determined by adjusting the original C_{gp} by an increment representing the percentage of change in calculated gross thrust necessary to make it equal to measured gross thrust (fig. 10). The data in figure 10 were obtained during the static ground thrust run and only provide information on this adjustment increment at low nozzle pressure ratios (p_{t_7}/p_{amb}). The trend of the data, however, shows how the adjustment increment should be extrapolated to the higher nozzle pressure ratios that are experienced in flight. The trend of the data in figure 10 shows that the percentage of change in the values approaches -5 percent; therefore, C_{gp} was reduced by 5 percent over the range of nozzle pressure ratios. The ground thrust data were then plotted using data that were calculated with the refaired values of C_{gp} and are given in figure 11.

Mass Momentum Method

A ground static thrust run was used to determine the coefficient C_f as a function of p_{t_7}/p_{amb} by using the following equations:

$$C_f = \frac{F_{g_m}}{A_8 \left[\left(\frac{2}{\gamma + 1} \right)^{\frac{\gamma}{\gamma - 1}} (\gamma + 1) p_{t_7} - p_{amb} \right]}$$

where $\gamma = 1.33$ and F_{g_m} is the measured thrust stand value of thrust.

The values of C_f obtained from the ground thrust run were plotted versus p_{t_7}/p_{amb} (fig. 4), and the resulting data were extrapolated out to the levels of p_{t_7}/p_{amb} available in flight. It was shown in reference 5 that C_f approaches a constant value at the higher values of p_{t_7}/p_{amb} . Therefore, based on an engineering evaluation of available data and the apparent logical extension of a curve fit through the data to the higher values of p_{t_7}/p_{amb} , the maximum C_f value was chosen to be 0.93.

Simplified Gross Thrust Method

The determination of the calculated parameter, p_{t_8} , includes an adjustment factor called K_2 , which appears in the following equation:

$$p_{t_F} = p_{t_7} \left\{ 1 - \left(\frac{\gamma_F}{\gamma_F - 1} \right) K_2 \left[\left(\frac{p_{t_7}}{p_{s_F}} \right) \frac{\gamma_F - 1}{\gamma_F} - 1 \right] \right\}$$

Because the only adjustment available to make calculated gross thrust equal measured gross thrust is p_{t_F} , and this variation must result from changes in K_2 , a plot of the variables p_{s_F} and p_{t_7} using ground thrust data is made. Figure 12 shows the values of K_2 required to make the percentage of error between measured and calculated gross thrust equal zero for given values of p_{s_F}/p_{t_7} . The data in this figure were obtained by first plotting constant values of K_2 to determine the variations of percent error between F_{g_m} , F_{g_c} , and p_{s_F}/p_{t_7} . When the values of gross thrust computed with the values of K_2 shown in figure 12 are used, the agreement between F_{g_c} and F_{g_m} is as shown in figure 13.

APPENDIX B.—DERIVATION OF SIMPLIFIED GROSS THRUST METHOD EQUATIONS

Equations for the calculation of the gross thrust of a simple, nonafterburning turbojet engine with a short tailpipe that use only measured parameters at the nozzle exit are derived below. This method is a modification of the SGTM, which was originally developed to calculate the thrust of a more complicated jet engine that incorporated such equipment as afterburners and ducted fans and is described in references 3 and 4.

In the material below the following assumptions are made. First, it is assumed that the exhaust nozzle is convergent only. Second, it is assumed that when

$$T_{t_7} \leq 700, \gamma_7 = 1.4$$

and that when

$$T_{t_7} > 700, \gamma_7 = 2.246409 \left(T_{t_7} \right)^{-0.070767} \quad (1)$$

Third, it is assumed that $\gamma_7 = \gamma_F = \gamma_8$. And finally, it is assumed that p_s is not actually measured at the nozzle exit (engine station 8) but at some point inside the nozzle exit we will call station F; therefore the pressures p_{s_F} and p_{t_F} and the area A_F all occur at engine station F.

The basic thrust equation in the SGTM is as follows:

$$F_g = C_{fg} \frac{\dot{m}_8 V_8}{g_0} + (p_{s_8} - p_{s_{amb}}) A_8 \quad (2)$$

where C_{fg} is the conventional gross thrust coefficient ($C_{fg} = 1$). Then

$$\dot{m}_8 = \dot{m}_F = \rho_F V_F A_F$$

where

ρ_F density at station F

V_F velocity at station F

A_F area at station F

The equation of state for the perfect gas is

$$p_{s_F} = \rho_F g_0 R_g T_{s_F}$$

where:

R_g gas constant, $8.314 \times 10^3 \text{ J kmol}^{-1} \text{ K}^{-1}$ ($53.35 \text{ ft-lbf/lbm-}^\circ\text{R}$)

g_0 gravitational constant, $6.6732 \times 10^{-11} \text{ N m}^2 \text{ kg}^{-2}$ ($32.17 \text{ ft-lb/lb-sec}^2$)

Then

$$\dot{m}_F = \frac{p_{s_F}}{g_0 R_g T_{s_F}} V_F A_F$$

For an unchoked engine, $p_{s_8} = p_{s_{\text{amb}}}$. Then, substituting values into equation (2),

$$\begin{aligned} F_g &= \frac{p_{s_F} V_F V_8 A_F}{g_0 R_g T_{s_F}} \\ &= \left(\frac{A_F}{g_0 R_g} \right) p_{s_F} \left(\frac{V_F}{\sqrt{T_{s_F}}} \right) \left(\frac{V_8}{\sqrt{T_{s_8}}} \right) \sqrt{\frac{T_{s_8}}{T_{s_F}}} \end{aligned}$$

If these equations are rewritten with $\frac{V}{\sqrt{\gamma g_0 R_g T_s}}$ and Mach number, M , equal to

$$\sqrt{\gamma g_0 R_g T_s}$$

$$F_g = \gamma F_A p_{s_F} M_F M_8 \sqrt{\frac{T_{s_8}}{T_{t_8}}} \sqrt{\frac{T_{t_F}}{T_{s_F}}} \quad (3)$$

Then, with $M = \sqrt{\frac{2}{\gamma - 1} \left[\left(\frac{p_t}{p_s} \right)^{\frac{\gamma - 1}{\gamma}} - 1 \right]}$ and $\frac{T_s}{T_t} = \left(\frac{p_s}{p_t} \right)^{\frac{\gamma - 1}{\gamma}}$ and $p_{s_8} = p_{\text{amb}}$ (unchoked) and $p_{t_F} = p_{t_8}$ (assumed),

$$F_g = \left(\frac{2\gamma_F}{\gamma_F - 1} \right) A_F p_{s_F} \left(\frac{p_{t_F}}{p_{s_F}} \right)^{\frac{\gamma_F - 1}{2\gamma_F}} \sqrt{\left(\frac{p_{t_F}}{p_{s_F}} \right)^{\frac{\gamma_F - 1}{\gamma_F}} - 1} \sqrt{1 - \left(\frac{p_{s_{amb}}}{p_{t_F}} \right)^{\frac{\gamma_F - 1}{\gamma_F}}} \quad (4)$$

$$\text{This is valid whenever } \frac{p_{t_F}}{p_{s_{amb}}} < \left(\frac{\gamma_F + 1}{2} \right)^{\frac{\gamma_F - 1}{\gamma_F - 1}}$$

For a choked engine the same derivation as for the unchoked engine is used but the pressure area term (eq. (3)) is carried along. The gross thrust equation would then be expressed as

$$F_g = \gamma_F A_F p_{s_F} M_F M_8 \sqrt{\frac{T_{s_8}}{T_{t_8}} \sqrt{\frac{T_{t_F}}{T_{s_F}}} + \left(p_{s_8} - p_{s_{amb}} \right) A_8}$$

Rewriting,

$$F_g = \gamma_F A_F p_{s_F} M_F M_8 \sqrt{\frac{T_{s_8}}{T_{t_8}} \sqrt{\frac{T_{t_F}}{T_{s_F}}} + p_{t_F} \left(\frac{p_{s_8}}{p_{t_F}} - \frac{p_{s_{amb}}}{p_{t_F}} \right) A_8}$$

$$\text{Then, with } M = \sqrt{\frac{2}{\gamma - 1} \left[\left(\frac{p_t}{p_s} \right)^{\frac{\gamma - 1}{\gamma}} - 1 \right]} \text{ and } \frac{T_s}{T_t} = \left(\frac{p_s}{p_t} \right)^{\frac{\gamma - 1}{\gamma}} \text{ and } M_8 = 1 \text{ (choked case),}$$

$$F_g = \gamma_F A_F p_{s_F} \sqrt{\frac{2}{\gamma_F - 1} \left[\left(\frac{p_{t_F}}{p_{s_F}} \right)^{\frac{\gamma_F - 1}{\gamma_F}} - 1 \right]} \left(\frac{p_{s_8}}{p_{t_8}} \right)^{\frac{\gamma_F - 1}{2\gamma_F}} \left(\frac{p_{t_F}}{p_{s_F}} \right)^{\frac{\gamma_F - 1}{2\gamma_F}} + p_{t_F} \left(\frac{p_{s_8}}{p_{t_F}} - \frac{p_{s_{amb}}}{p_{t_F}} \right) A_8 \quad (5)$$

For the choked case where $M_8 = 1$, then

$$\left(\frac{p_{s_8}}{p_{t_8}}\right)^{\frac{\gamma_F - 1}{2\gamma_F}} = \left[\left(\frac{2}{\gamma_F + 1}\right)^{\frac{\gamma_F - 1}{\gamma_F + 1}}\right]^{\frac{\gamma_F - 1}{2\gamma_F}} = \left(\frac{2}{\gamma_F + 1}\right)^{1/2}$$

Rearranging (assuming that $p_{t_F} = p_{t_8}$),

$$F_g = \left(\frac{2\gamma_F}{\gamma_F - 1}\right) A_F p_{s_F} \left\{ \sqrt{\frac{\gamma_F - 1}{2}} \sqrt{\frac{2}{\gamma_F + 1}} \sqrt{\left[\left(\frac{p_{t_F}}{p_{s_F}}\right)^{\frac{\gamma_F - 1}{\gamma_F}} - 1 \right]} \left(\frac{p_{t_F}}{p_{s_F}}\right)^{\frac{\gamma_F - 1}{2\gamma_F}} \right. \\ \left. + \left(\frac{p_{t_F}}{p_{s_F}}\right) \left(\frac{\gamma_F - 1}{2\gamma_F}\right) \left[\left(\frac{2}{\gamma_F + 1}\right)^{\frac{\gamma_F - 1}{\gamma_F + 1}} - \frac{p_{s_{amb}}}{p_{t_F}} \right] \frac{A_8}{A_F} \right\} \quad (6)$$

From reference 6 (p. 86, eq. 4-19),

$$\frac{A_F}{A_8} = \frac{1}{M_F} \left[\left(\frac{2}{\gamma_F - 1}\right) \left(1 + \frac{\gamma_F - 1}{2} M_F^2\right) \right]^{\frac{\gamma_F + 1}{2(\gamma_F - 1)}}$$

Since

$$M_F^2 = \frac{2}{\gamma_F - 1} \left[\left(\frac{p_{t_F}}{p_{s_F}}\right)^{\frac{\gamma_F - 1}{\gamma_F}} - 1 \right]$$

then

$$A_8 = A_F \sqrt{\frac{2}{\gamma_F - 1} \left[\left(\frac{p_{t_F}}{p_{s_F}}\right)^{\frac{\gamma_F - 1}{\gamma_F}} - 1 \right]} \left(\frac{\gamma_F + 1}{2}\right)^{\frac{\gamma_F + 1}{2(\gamma_F - 1)}} \left(\frac{p_{t_F}}{p_{s_F}}\right)^{\frac{-(\gamma_F + 1)}{2\gamma_F}}$$

Substituting into equation (6) and rearranging yields

$$\begin{aligned}
 F_g = & \left(\frac{2\gamma_F}{\gamma_F - 1} \right) A_F p_{s_F} \sqrt{\left[\left(\frac{p_{t_F}}{p_{s_F}} \right)^{\frac{\gamma_F - 1}{\gamma_F}} - 1 \right]} \left(\frac{p_{t_F}}{p_{s_F}} \right)^{\frac{\gamma_F - 1}{2\gamma_F}} \left\{ \sqrt{\frac{\gamma_F - 1}{\gamma_F + 1}} \right. \\
 & \left. + \frac{\sqrt{\frac{\gamma_F - 1}{2}}}{\gamma_F} \left[\left(\frac{2}{\gamma_F + 1} \right)^{\frac{\gamma_F}{\gamma_F - 1}} - \frac{p_{s_{amb}}}{p_{t_F}} \right] \left(\frac{\gamma_F + 1}{2} \right)^{\frac{\gamma_F + 1}{2(\gamma_F - 1)}} \right\}
 \end{aligned} \tag{7}$$

To get p_{t_F} , we look at reference 6 (table 8.2), and see that

$$\frac{dp_t}{p_t} = 0 \frac{dA}{A} - \frac{\gamma_M^2}{2} \frac{dT_t}{T_t} - \frac{\gamma_M^2}{2} \frac{dM}{M} - \gamma_M^2 \frac{d\omega}{\omega}$$

where

$\frac{dp_t}{p_t}$ total pressure change term

$\frac{dA}{A}$ cross-sectional area change term

$\frac{dT_t}{T_t}$ total temperature change term

$\frac{dM}{M}$ momentum change term of "frictional effects"

$\frac{d\omega}{\omega}$ mass flow change term

For this engine (J57-P-43W), assume that between engine station 7 and station F

$$\frac{dT_t}{T_t} = \frac{d\omega}{\omega} = 0$$

which leaves

$$\frac{dp_t}{p_t} \Bigg|_{7-F} = -\frac{\gamma M^2}{2} \frac{dM}{M} \Bigg|_{7-F} \cong \frac{p_{t_F} - p_{t_7}}{p_{t_7}}$$

The representative Mach number is assumed to be a function of p_{t_7} and p_{t_F} , written as follows:

$$M^2 = \frac{2}{\gamma - 1} \left[\left(\frac{p_{t_7}}{p_{s_F}} \right)^{\frac{\gamma - 1}{\gamma}} - 1 \right]$$

then, letting $K_2 = \frac{dM}{M} \Big|_{7-F}$ and rearranging,

$$p_{t_F} = p_{t_7} \left\{ 1 - \frac{\gamma_F}{\gamma_F - 1} K_2 \left[\left(\frac{p_{t_7}}{p_{s_F}} \right)^{\frac{\gamma_F - 1}{\gamma_F}} - 1 \right] \right\} \quad (8)$$

The assumptions here are that equation (1) can be used to determine γ ; molecular weight is constant; flow is one dimensional; heat transfer is zero; a representative Mach number, M , can be used; $M = f(p_{t_7}, p_{s_F})$; mass flow change is zero; and K_2 is constant.

Calibration is accomplished by using equations (4), (7), and (8), iterating against the value of F_g obtained on the thrust stand, seeking a constant K_2 .

REFERENCES

1. General Military Turbojet Installation Handbook. Pratt & Whitney Aircraft, Inc., July 1958. (Available from Pratt & Whitney Aircraft Group, Government Products Div., P.O. Box 2691, West Palm Beach, Fla. 33402.)
2. Beeler, De E.; Bellman, Donald R.; and Saltzman, Edwin J.: Flight Techniques for Determining Airplane Drag at High Mach Number. NACA TN 3821, 1956.
3. Kurtenbach, Frank J.: Comparison of Calculated and Altitude-Facility-Measured Thrust and Airflow of Two Prototype F100 Turbofan Engines. NASA TP-1373, 1978.
4. Kurtenbach, Frank J.: Evaluation of a Simplified Gross Thrust Calculation Technique Using Two Prototype F100 Turbofan Engines in an Altitude Facility. NASA TP-1482, 1979.
5. Herrington, Russel M.; Shoemacher, Paul E.; Bartlett, Eugene P.; and Dunlap, Everett W.: Flight Test Engineering Handbook. Tech. Rept. No. 6273, Air Force Flight Test Center, May 1951 (rev. June 1964).
6. Shapiro, Ascher H.: The Dynamics and Thermodynamics of Compressible Fluid Flow, Vol. I. The Ronald Press Co., c.1953.

TABLE 1.—FLIGHT DATA STABILIZED TEST CONDITIONS

Flight number	Maneuver number	Mach number	Altitude, m (ft)	Dynamic pressure, N/m ² (psf)	W/S, kg (lb)
21	1	0.703 0.750 0.784 0.798 0.819	11,290 (37,040) 11,348 (37,230) 11,467 (37,620) 11,665 (38,270) 11,814 (38,670)	3.258 (156) 3.676 (176) 3.947 (189) 3.968 (190) 4.094 (196)	476,272 (1,050,000)
22	2	0.706 0.737 0.774 0.794 0.816	11,445 (37,550) 11,378 (37,330) 11,345 (37,220) 11,311 (37,110) 11,265 (36,960)	3.216 (154) 3.530 (169) 3.926 (188) 4.156 (199) 4.428 (212)	476,272 (1,050,000)
23	3	0.619 0.766 0.773 0.802 0.817	11,311 (37,110) 11,192 (36,720) 11,207 (36,770) 11,177 (36,670) 11,086 (36,370)	3.133 (150) 3.926 (188) 4.010 (192) 4.323 (207) 4.553 (218)	362,874 (800,000)
23	4	0.702 0.756 0.777 0.790 0.814	10,875 (35,680) 10,817 (35,490) 10,744 (35,250) 10,714 (35,150) 10,631 (34,880)	3.467 (166) 4.073 (195) 4.344 (208) 4.511 (216) 4.845 (232)	408,233 (900,000)
25	5	0.700 0.741 0.766 0.790	10,583 (34,720) 10,482 (34,390) 10,409 (34,150) 10,357 (33,980)	3.613 (173) 4.114 (197) 4.428 (212) 4.762 (228)	362,874 (800,000)

Flight number	Maneuver number	Mach number	Altitude, m (ft)	Dynamic pressure, N/m ² (psf)	W/S, kg (lb)
25	6	0.694 0.745 0.770 0.790 0.814	10,628 (34,870) 10,589 (34,740) 10,574 (34,690) 10,519 (34,519) 10,409 (34,150)	3.530 (169) 4.094 (196) 4.386 (210) 4.657 (223) 5.013 (240)	408,233 (900,000)
25	7	0.709 0.760 0.781 0.802 0.818	11,232 (36,850) 11,101 (36,420) 11,009 (36,120) 10,994 (36,070) 10,836 (35,550)	3.342 (160) 3.926 (188) 4.219 (202) 4.449 (213) 4.741 (227)	476,272 (1,050,000)
27	8	0.695 0.744 0.769 0.787 0.809	10,769 (35,330) 10,662 (34,980) 10,519 (34,510) 10,467 (34,340) 10,394 (34,100)	3.470 (166) 4.031 (193) 4.407 (211) 4.657 (223) 4.950 (237)	362,874 (800,000)
27	9	0.697 0.740 0.771 0.791 0.812	10,683 (35,050) 10,616 (34,830) 10,567 (34,670) 10,430 (34,220) 10,342 (33,930)	3.530 (169) 4.031 (193) 4.407 (211) 4.741 (227) 5.033 (241)	408,233 (900,000)
27	10	0.694 0.751 0.784 0.805 0.816	11,226 (36,830) 11,131 (36,520) 11,049 (36,250) 10,958 (35,950) 10,894 (35,740)	3.216 (154) 3.822 (183) 4.219 (202) 4.511 (216) 4.678 (224)	476,272 (1,050,000)

TABLE 2.—INSTRUMENTATION CHARACTERISTICS AND MEASUREMENT PRECISION

(a) Pressure instrumentation characteristics

Pressure measured	Sensor type	Sensor range, kN/m ² (lb/in ²)
p_{amb}	Absolute	0 to -13.8 (0 to 20)
p_{t_2}	Differential	$\pm 27.6 (\pm 4)$
$p_{t_2}^{ref}$	Differential	0 to 276 (0 to 40)
p_{t_7}	Differential	0 to 276 (0 to 40)
p_{s_F}	Differential	$\pm 207 (\pm 30)$

(b) Measurement precision

	Maximum error
M_∞ , percent of value	± 1
h , m (ft)	$\pm 33.5 (\pm 110)$
p_{amb} , kN/m ² , percent of full scale	± 0.05
p_{t_2} , kN/m ² , percent of full scale	± 2
$p_{t_2}^{ref}$, kN/m ² , percent of full scale	± 0.05
p_{t_7} , kN/m ² , percent of full scale	± 2
p_{s_F} , kN/m ² , percent of full scale	± 2
T_t , deg	± 10
T_{t_7} , deg	± 4
$N_1/\sqrt{\theta_{t_2}}$, rpm	± 10

TABLE 3.—COMPARISON OF THRUST CALCULATION PARAMETERS

Gas generator method		Mass momentum method		Simplified gross thrust method	
	Parameter—	Parameter—	Function of—	Parameter—	Function of—
Variables	ψ	(p_{t_7}/p_{amb}) , γ	-----	-----	γ_F
	γ	T_{t_7}	-----	-----	p_{t_F}
Coefficients	C_{gp}	p_{t_7}/p_{amb}	C_f	p_{t_7}/p_{amb}	K_2
Measured parameters	p_{t_7} , p_{amb} , T_{t_7}		p_{t_7} , p_{amb}		p_{t_7} , p_{amb} , T_{t_7} , p_{s_F}
Constants	A_8		A_8 , γ		A_8 , A_F
Final expression	$F_g = \psi p_{amb} C_{gp} A_8$		$F_g = C_f A_8 \left[\left(\frac{2}{\gamma + 1} \right)^{\frac{\gamma}{\gamma - 1}} (\gamma + 1) p_{t_7} - p_{amb} \right]$		$F_g = \left(\frac{2\gamma_F}{\gamma_F - 1} \right) A_F p_{s_F} \sqrt{\left[\left(\frac{p_{t_F}}{p_{s_F}} \right)^{\frac{\gamma_F - 1}{\gamma_F}} - 1 \right]} \left(\frac{p_{t_F}}{p_{s_F}} \right)^{\frac{\gamma_F - 1}{2\gamma_F}} \left\{ \sqrt{\frac{\gamma_F - 1}{\gamma_F + 1}} \right.$ $+ \left. \sqrt{\frac{\gamma_F - 1}{2}} \left[\left(\frac{2}{\gamma_F + 1} \right)^{\frac{\gamma_F}{\gamma_F - 1}} - \frac{p_{s_{amb}}}{p_{t_F}} \right] \left(\frac{\gamma_F + 1}{2} \right)^{\frac{\gamma_F + 1}{2(\gamma_F - 1)}} \right\}$

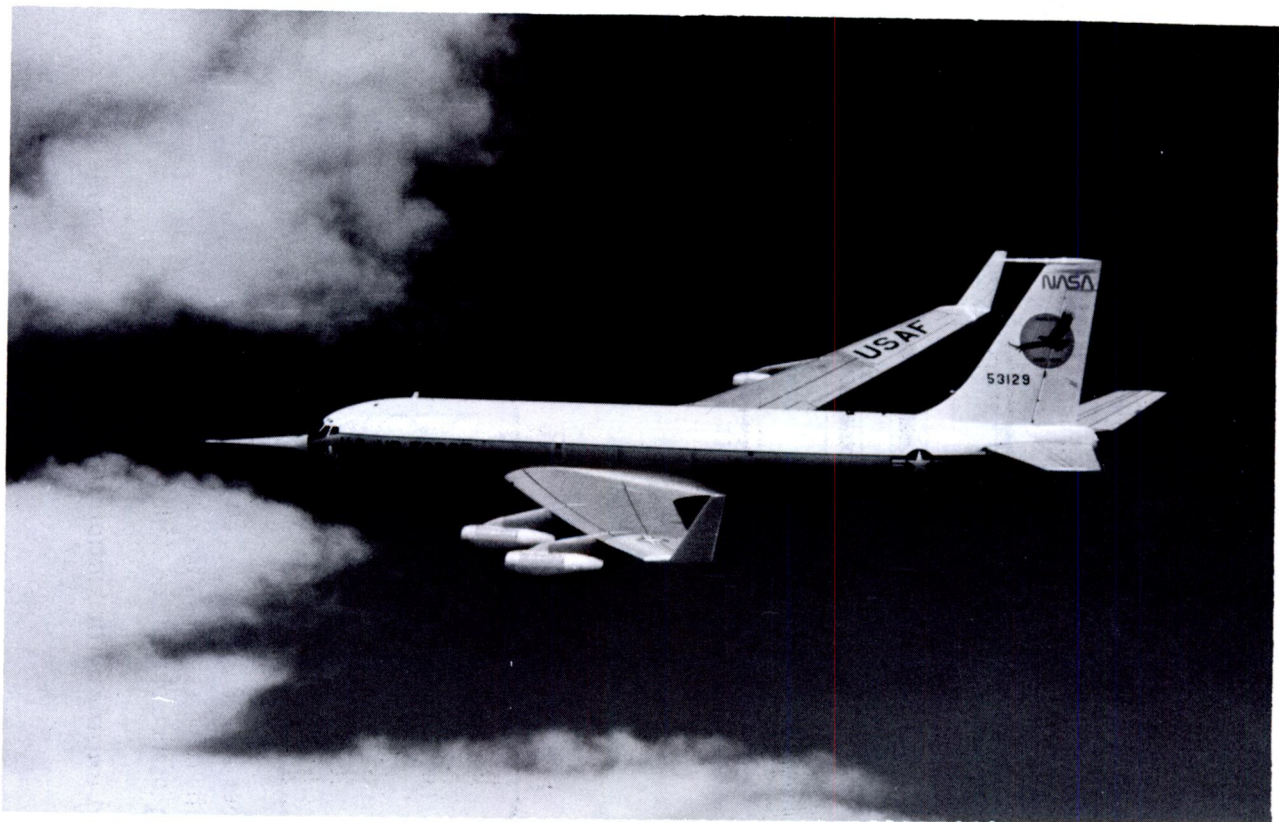


Figure 1. KC-135A aircraft modified with winglets.

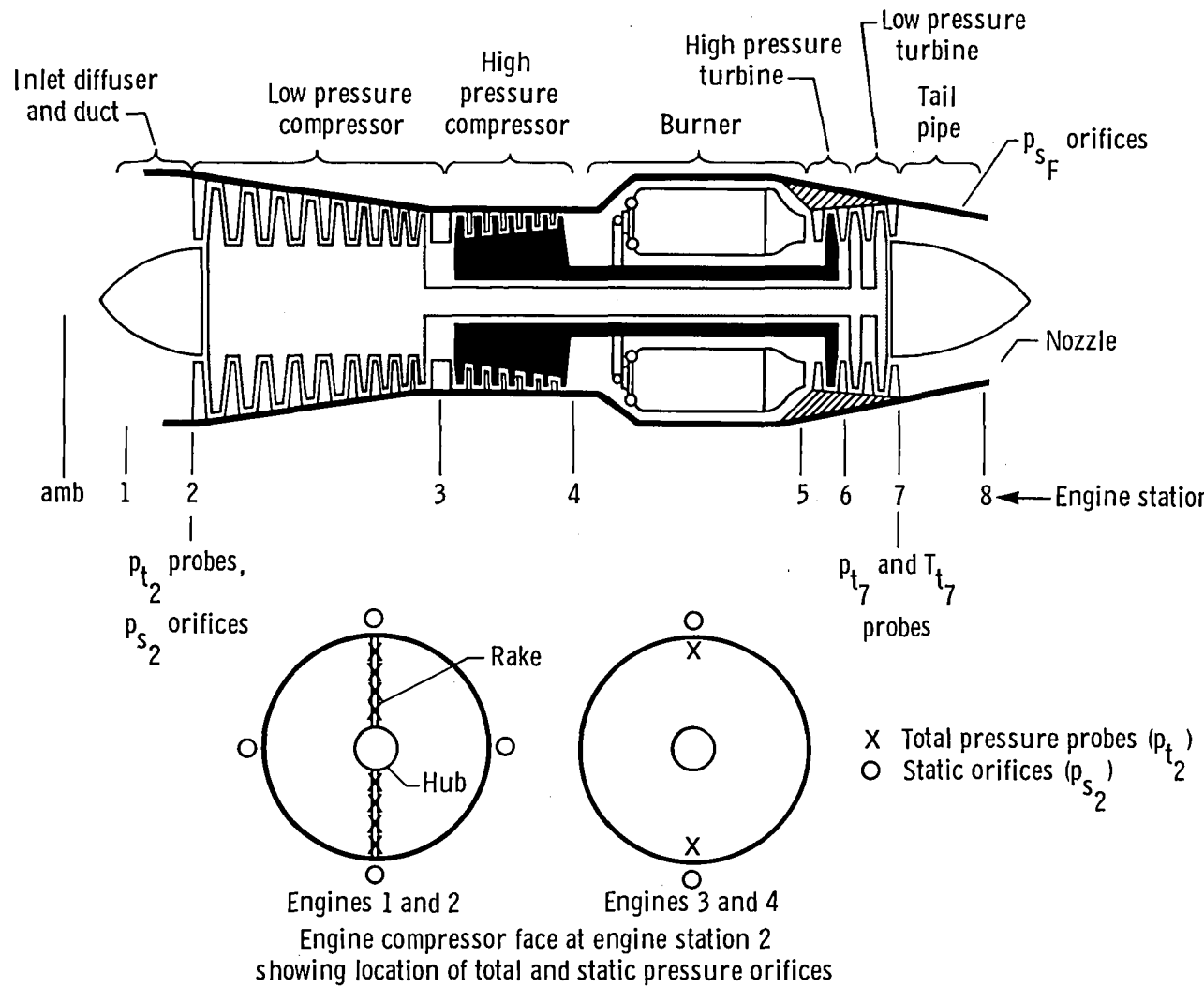


Figure 2. J57-P-43W turbofan engine with station designations and measured parameter locations.

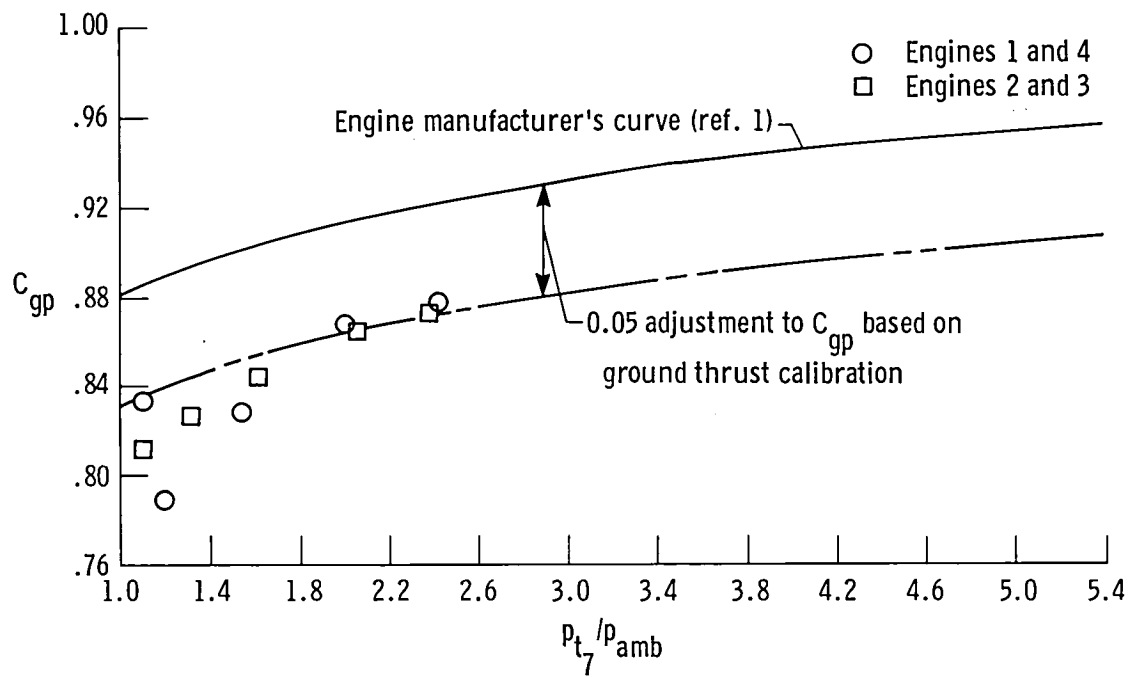


Figure 3. Turbojet nozzle gross thrust coefficient.

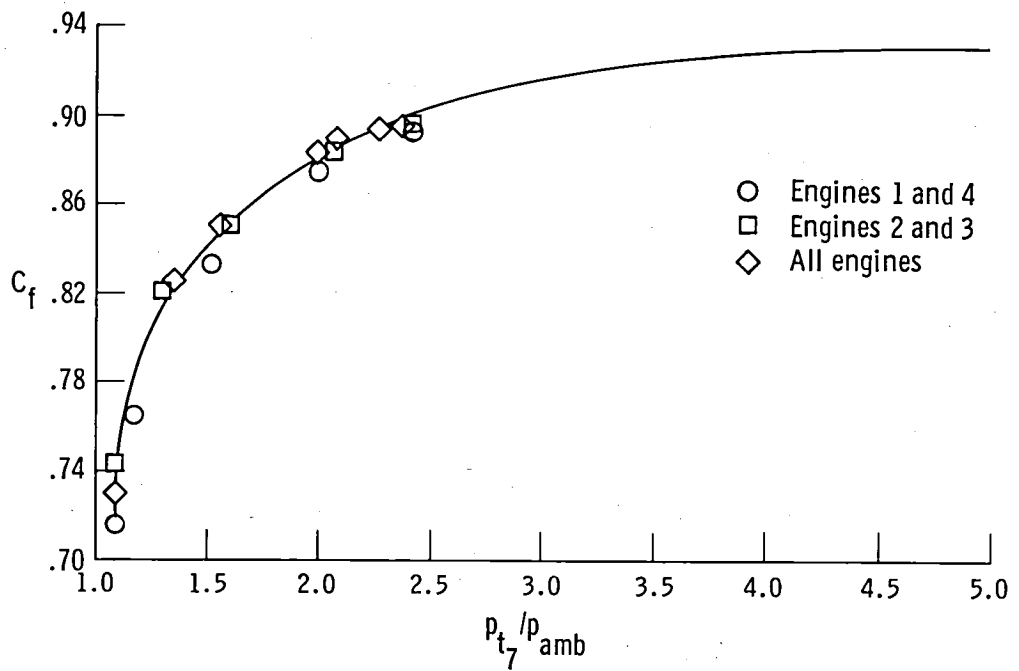


Figure 4. Nozzle coefficient determined by ground thrust calibration.

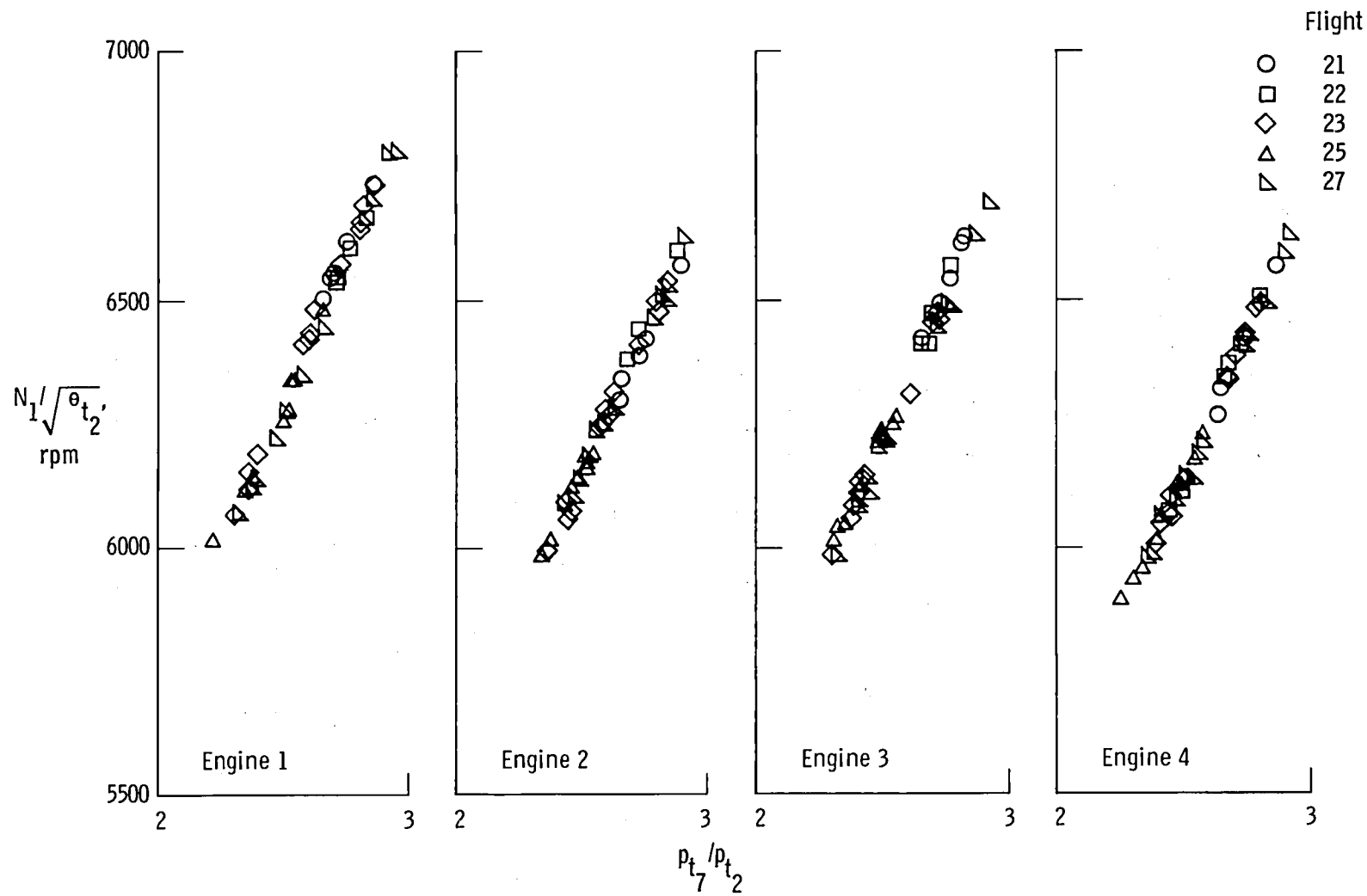


Figure 5. Condition of J57-P-43W engines during flight test program.

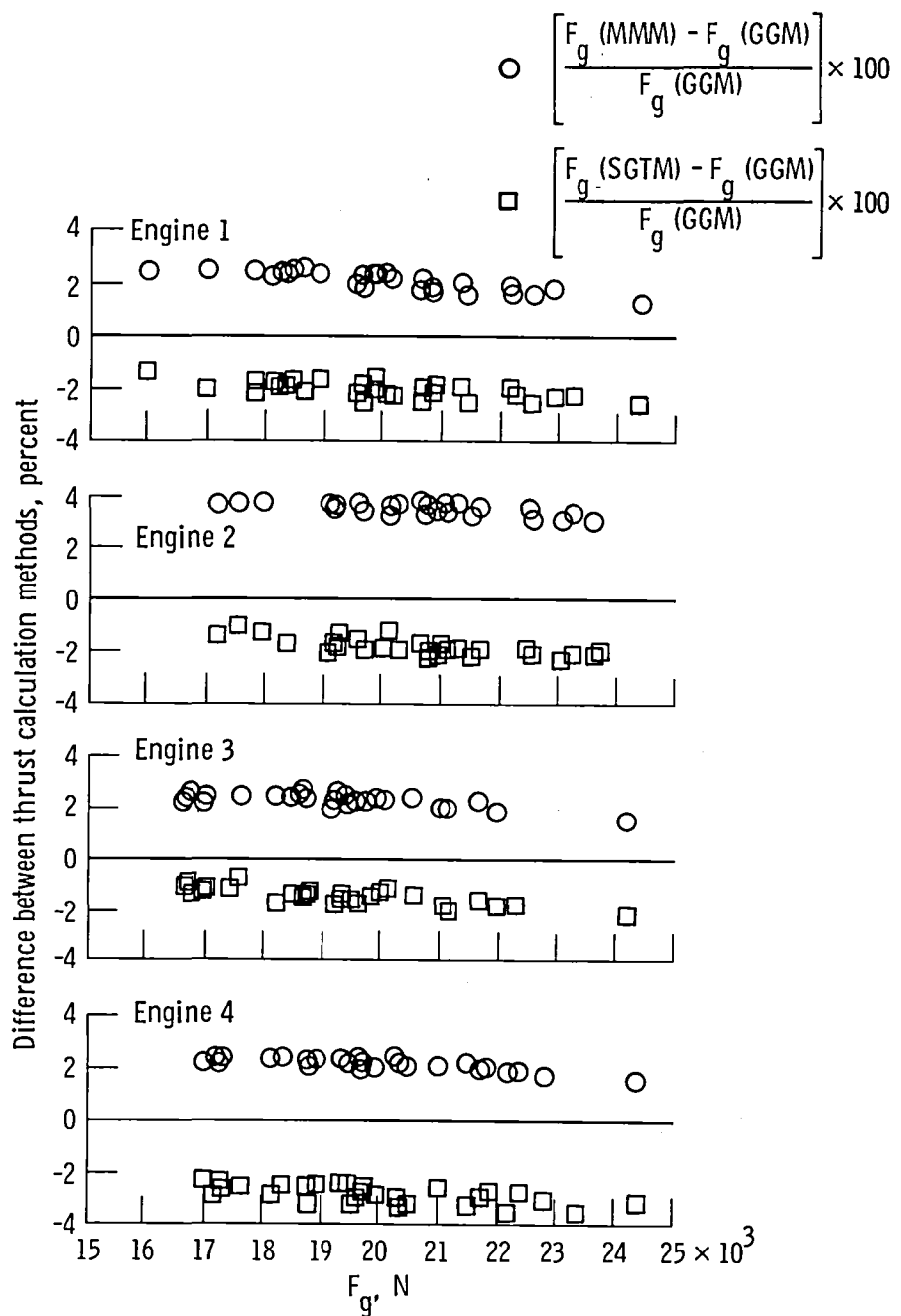


Figure 6. Comparison of calculated gross thrust values for each engine.

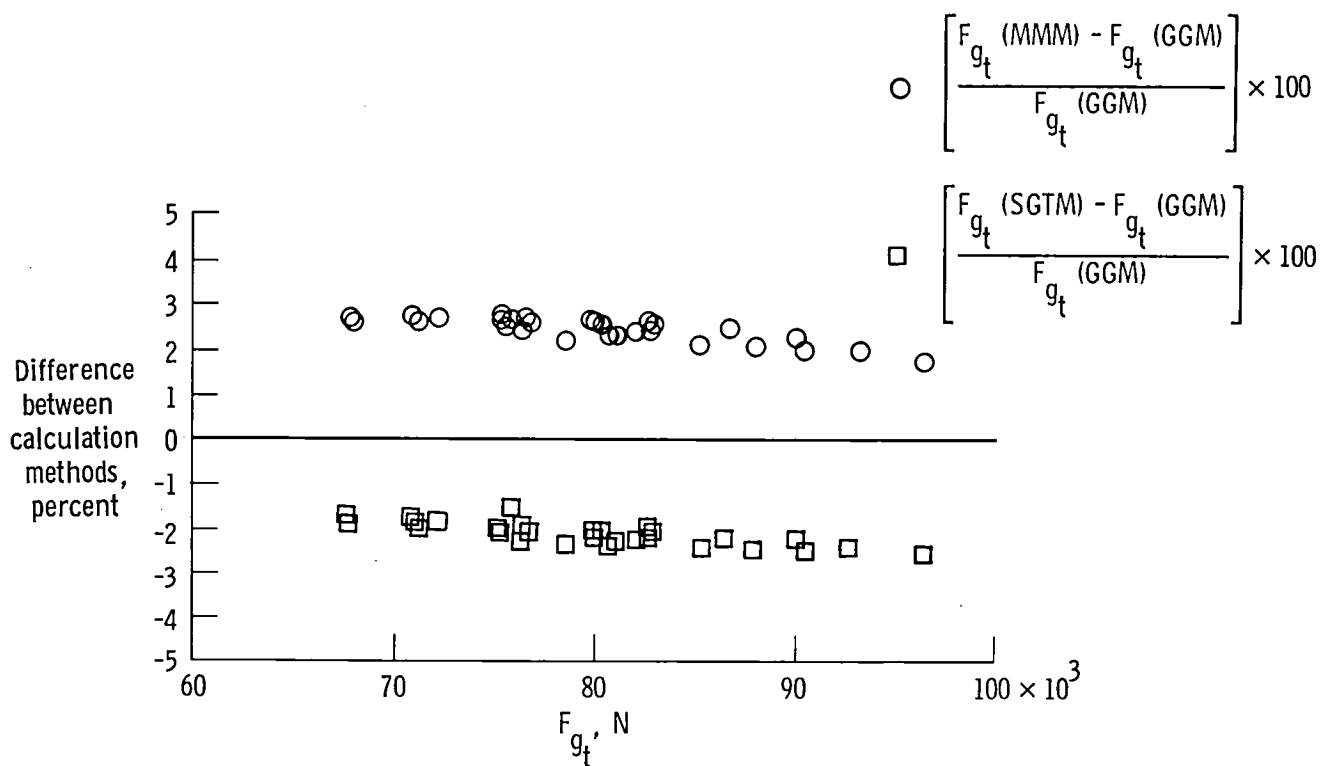


Figure 7. Comparison of total aircraft gross thrust values (all engines).

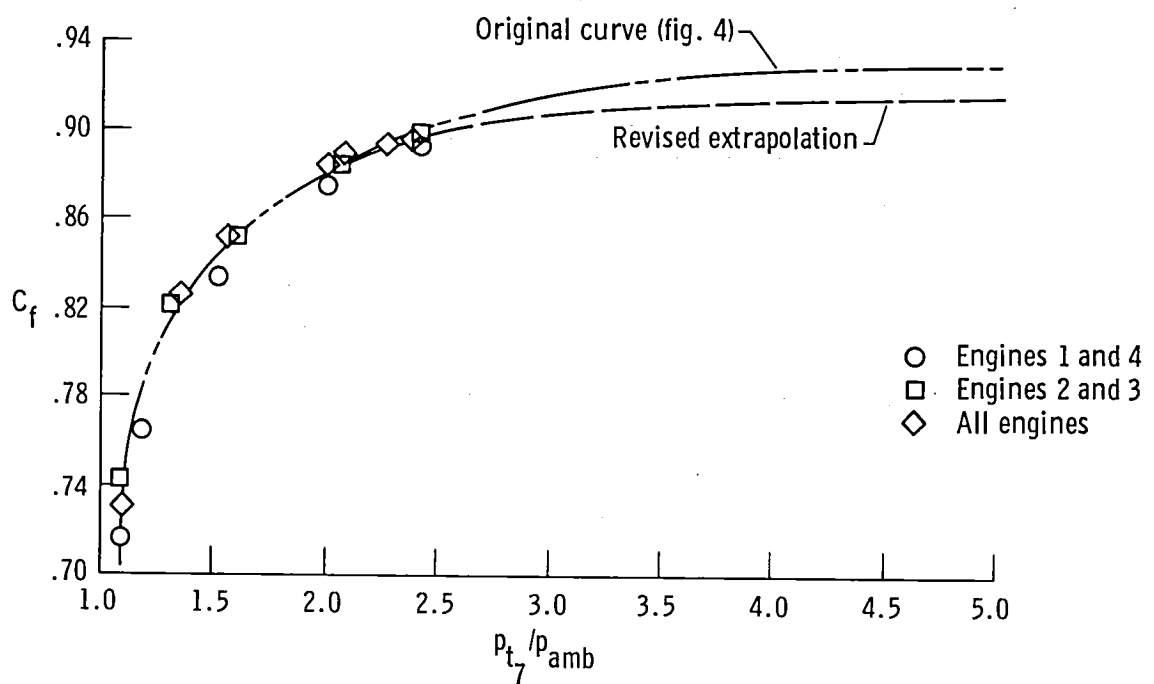


Figure 8. Revised extrapolation of C_f for MMM.

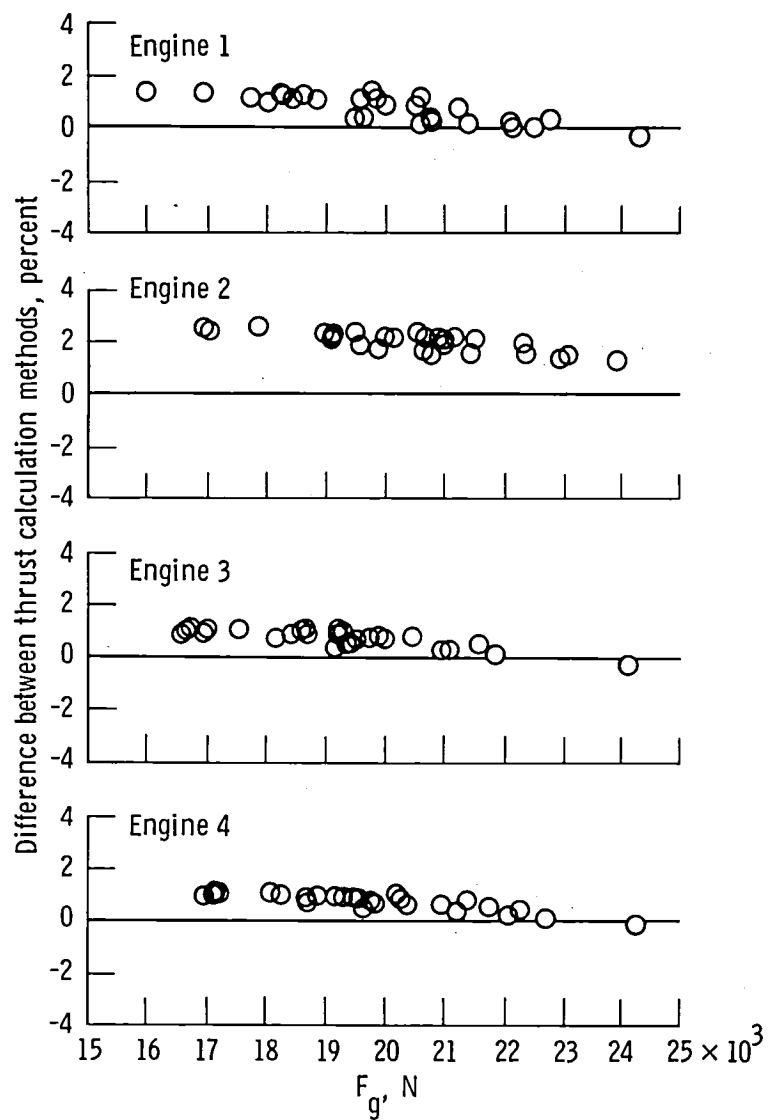


Figure 9. Comparisons of calculated gross thrust values using revised C_f extrapolation. Values

represent $\left[\frac{F_g(\text{MMM}) - F_g(\text{GGM})}{F_g(\text{GGM})} \right] \times 100$.

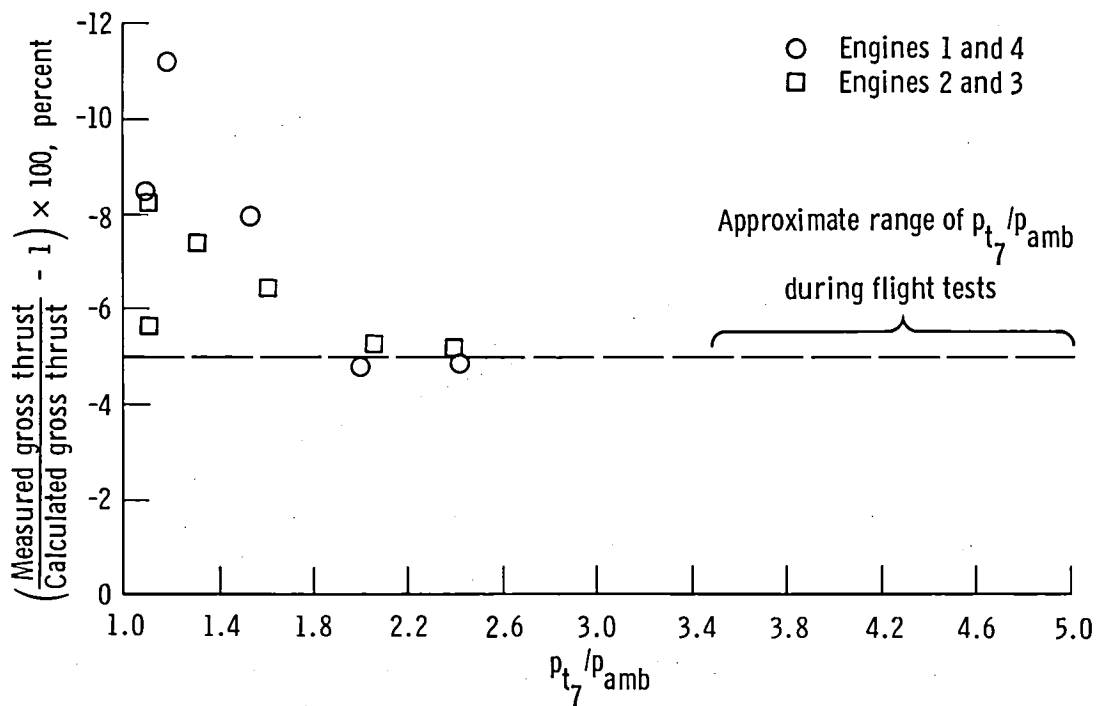


Figure 10. Percentage of change required to make calculated gross thrust equal measured gross thrust for the GGM during ground calibration.

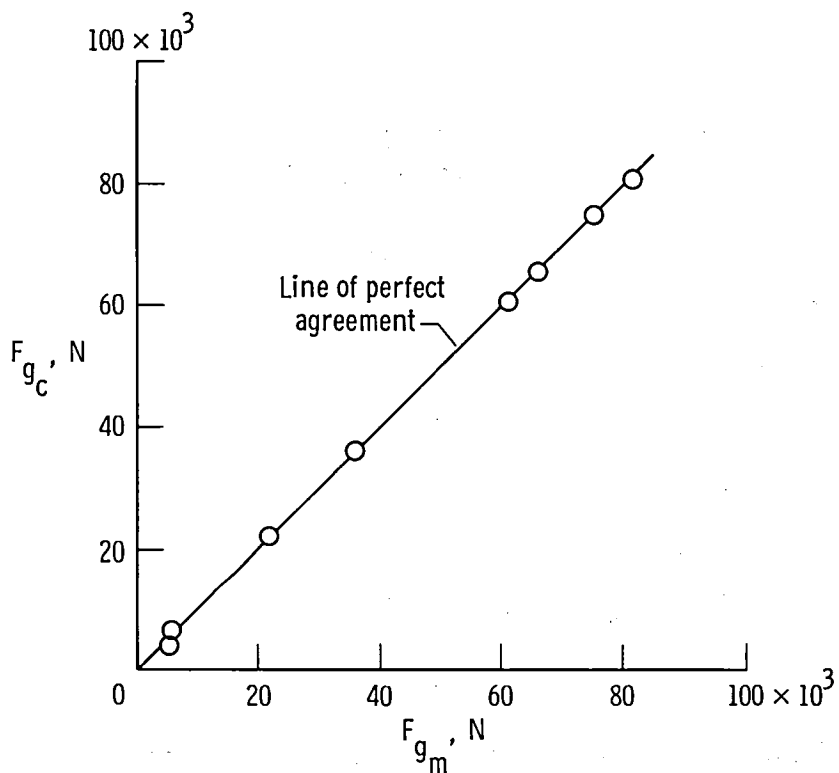


Figure 11. Comparison of calculated and measured gross thrust after calibration adjustment of C_{gp} curve. GGM.

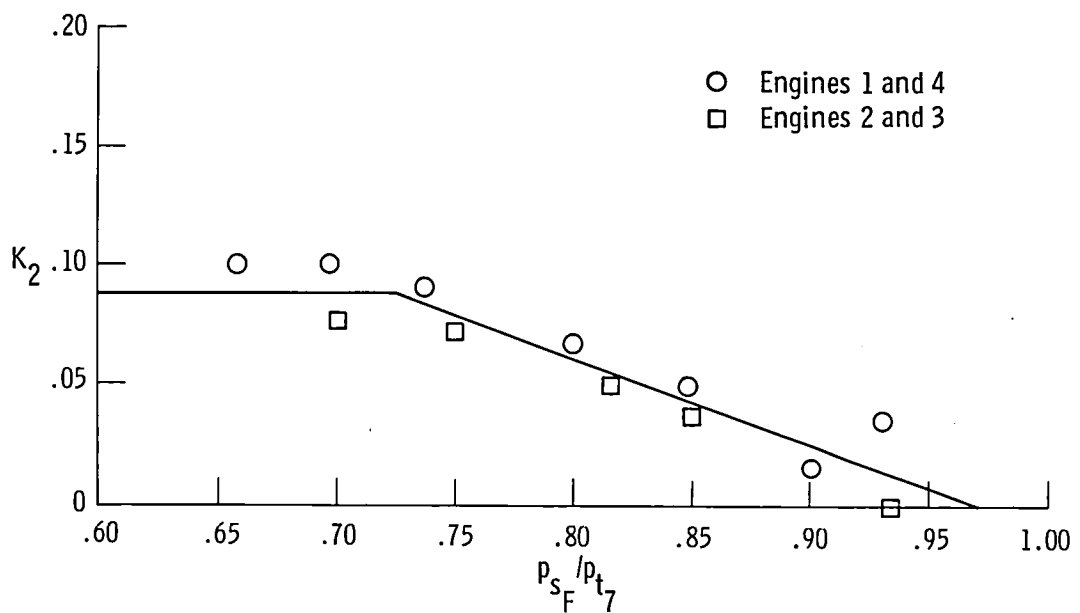


Figure 12. Parameter relationships required to make F_{g_c} equal to F_{g_m} for SGTM.

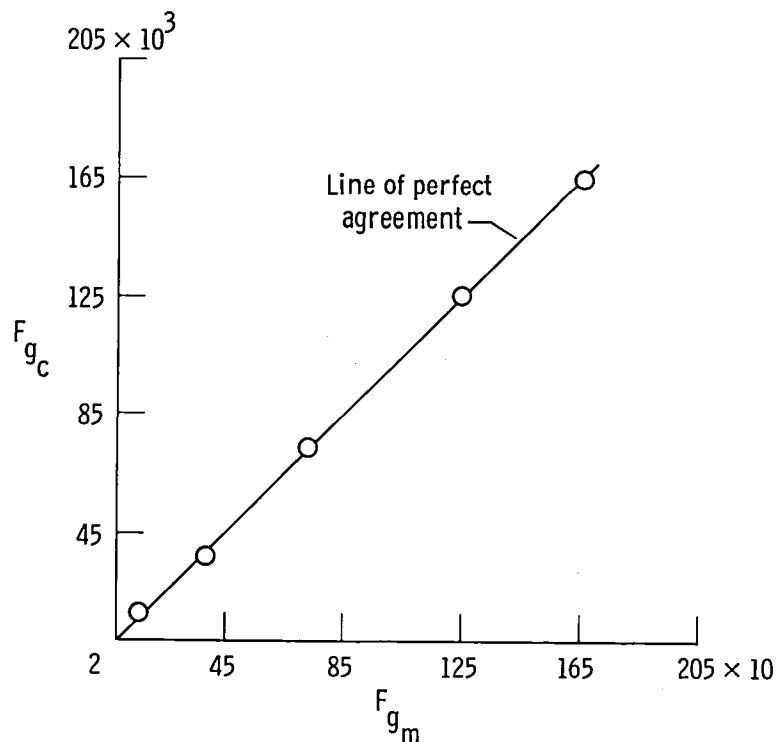


Figure 13. Comparison of calculated and measured gross thrust after calibration adjustment. SGTM.

1. Report No. NASA TM-81360	2. Government Accession No.	3. Recipient's Catalog No.	
4. Title and Subtitle COMPARISON OF THREE THRUST CALCULATION METHODS USING IN-FLIGHT THRUST DATA		5. Report Date July 1981	
7. Author(s) Donald L. Hughes		6. Performing Organization Code 534-02-14	
9. Performing Organization Name and Address NASA Dryden Flight Research Center P.O. Box 273 Edwards, California 93523		8. Performing Organization Report No. H-1141	
12. Sponsoring Agency Name and Address National Aeronautics and Space Administration Washington, D.C. 20546		10. Work Unit No.	
		11. Contract or Grant No.	
		13. Type of Report and Period Covered Technical Memorandum	
		14. Sponsoring Agency Code	
15. Supplementary Notes			
16. Abstract The gross thrust of an experimental airplane was determined by three different but not totally independent methods of calculation using the same flight maneuvers and generally the same data parameters. Coefficients determined from thrust stand calibrations for each of the three methods were then extrapolated to cruise flight conditions. The values of total aircraft gross thrust calculated by the three methods for cruise flight conditions agreed within ± 3 percent. The disagreement in the values of thrust calculated by the different techniques manifested itself as a bias in the data. There was little scatter (± 0.5 percent) for the thrust levels examined in flight.			
17. Key Words (Suggested by Author(s)) Thrust calculations In-flight thrust		18. Distribution Statement Unclassified-Unlimited	
STAR category 05			
19. Security Classif. (of this report) Unclassified	20. Security Classif. (of this page) Unclassified	21. No. of Pages 35	22. Price* A03

*For sale by the National Technical Information Service, Springfield, Virginia 22161

National Aeronautics and
Space Administration

Washington, D.C.
20546

Official Business

Penalty for Private Use, \$300

THIRD-CLASS BULK RATE

Postage and Fees Paid
National Aeronautics and
Space Administration
NASA-451



NASA

POSTMASTER: If Undeliverable (Section 158
Postal Manual) Do Not Return
